

Flight Test Results: CTAS and FMS Cruise/Descent Trajectory Prediction Accuracy

Steven M. Green
Manager, En route Systems
NASA Ames Research Center
Moffett Field, California 94035
sgreen@mail.arc.nasa.gov

Michael P. Grace
Software Engineer
Raytheon
Moffett Field, California 94035
mgrace@mail.arc.nasa.gov

David H. Williams
Aerospace Engineer
NASA Langley Research Center
Hampton, Virginia 23681-2199
d.h.williams@larc.nasa.gov

Abstract

Two flight tests were conducted, using the Center TRACON Automation System (CTAS) and a Boeing 737 research airplane, to study trajectory-prediction accuracy. Four levels of cockpit automation were evaluated to study the influence of avionics on trajectory predictability. 48 descent runs were analyzed, using radar and satellite-navigation data to measure CTAS and Flight-Management-System (FMS) prediction accuracy and error sources. Mean arrival-time-prediction errors (CTAS and FMS) were less than 15 sec with standard deviations less than 13 sec. The dominant error source was the predicted winds aloft. CTAS airplane-performance-model errors did not contribute significantly to arrival-time error, but did affect vertical-profile-prediction accuracy. Although errors in radar-based position and velocity estimates had no significant influence on test results, significant errors in the velocity estimates were measured during turns. The most significant effect related to cockpit automation was a turn-overshoot error associated with unequipped, "classic" airplanes. (FMS-lateral-navigation (LNAV) guidance eliminated such error.) Pilot procedures and vertical guidance were also found to significantly reduce the vertical-profile error associated with errors in CTAS atmospheric and performance models.

Introduction

Air Traffic Management (ATM) research at NASA has led to the creation of the Center-TRACON Automation System (CTAS). CTAS is designed with the long-term goal of integration with airspace-user automation, including avionics such as Flight Management Systems (FMS). The objective is to maximize user flexibility, traffic throughput, and ATM and user productivity.

Trajectory-prediction accuracy directly influences the effectiveness and efficiency of ATM decision support tool (DST) advisories for flow-rate conformance (e.g., arrival metering), separation assurance, and vertical profile planning. Improved accuracy benefits the system by reducing conflict-prediction uncertainties and the need for excess separation buffers. In addition, advanced concepts that integrate FMS and ATM-DST capabilities depend on the relative accuracy of both systems. Relative accuracy not only influences the performance of air-traffic services, but also impacts the requirements for defining globally-interoperable avionics that depend on, among other things, the compatibility of FMS and ATM DSTs.

The transition to and from terminal airspace is a key challenge. Although accurate predictions may be relatively easy for straight-and-level flight, transition trajectories involve significant changes in course, altitude, and/or speed. Efficient transition trajectories depend on the planning and execution of smooth paths with minimal deviation (i.e., efficient 4D management).

FMS and ATM DST technologies have developed, for the most part, independently. An FMS is designed to help a pilot plan and fly a user-efficient flight profile that satisfies performance restrictions and operational constraints. In contrast, ATM DSTs must plan for multiple aircraft interactions to schedule arrivals, ensure separation, and provide suggested speed, altitude, and routing clearances to maximize throughput.

Early piloted-simulation tests of ATM trajectory-prediction algorithms demonstrated favorable results in terms of meter-fix arrival-time accuracy [1, 2]. Supplementary tests were needed to evaluate accuracy under realistic field conditions, including the errors associated with radar tracking, aircraft-performance modeling, and atmospheric (winds-aloft) prediction.

Two flight tests were conducted at the Denver Center to validate ATM DST and FMS trajectory predictions. This paper describes these tests and summarizes the results in terms of 4D trajectory-prediction accuracy and error sources. Although the data set (48 runs) is not large enough to be statistically significant, the results provide insight into real-world accuracy and error sources.

Center - TRACON Automation System

CTAS is an integrated suite of ATM DSTs that assist controllers with computer-generated information and advisories [3]. The CTAS En route Descent Advisor (EDA) is an en route DST that automatically updates 4D predictions for all aircraft in the climb, cruise, and descent phases of flight. EDA algorithms for flow-rate conformance and conflict detection and resolution (CD&R) provide controllers with clearance advisories that minimize deviations from the user's preferred trajectories. EDA advisories are particularly useful for high-density arrival metering, en route spacing, and the merging of departures into en route streams.¹ A detailed description of the EDA concept, functional overview, and benefits may be found in [4].

¹ A near-term spin-off capability, called Direct-To (D2), is currently undergoing field trials. D2 provides the controller with flight-path shortcut advisories and an interface to minimize workload.

EDA Trajectory Prediction Process

4D trajectory predictions form the cornerstone of CTAS/EDA. Trajectory predictions are generated based on aircraft state, flight-path intent, aircraft-performance models, and predicted atmospheric state (winds and temperatures aloft). The initial position, velocity and altitude of each flight are estimated from the best source available (flight plan, radar track, or data link). The flight-path intent is defined as a series of waypoints defining the path to the destination. This intent is based on the aircraft's current state, flight plan, local Air-Traffic-Control (ATC) procedures, and CTAS heuristics that relate the aircraft's current state to the flight plan and local procedures. The local procedures are defined in a CTAS navigation database in terms of altitude, airspeed, and course restrictions. Special functions and a controller-friendly graphical user interface ensure that EDA predictions are consistent with controller intent.

CTAS trajectories are synthesized in two steps. First, a horizontal track is generated by connecting the waypoints with a series of straight-line and circular turn segments. As for an FMS, waypoints are modeled as either "fly-by" or "fly-over" according to local airspace adaptation data. The turn segments are based on a parameterized bank angle and an estimated average ground-speed for the turn. This ground-speed is based on an airspeed profile and a wind estimate along a simple kinematic altitude profile. The airspeed profile is either inferred from a combination of the flight plan, controller input, radar tracking, and the CTAS database, or dynamically selected by EDA for flow-rate-conformance advisories. Second, the altitude and time profiles are computed by integrating a set of simplified point-mass equations of motion along the established ground track. A detailed set of aircraft-performance models are used to define the thrust, drag, and speed envelope for each aircraft type. The atmosphere is modeled with a 3D grid of wind, temperature, and pressure [5]. A detailed description of the CTAS trajectory-synthesis process is presented in [6].

Flight Test Experiment Description

Objective

The primary objective of the flight test was to validate CTAS and FMS trajectory-prediction accuracy and identify and measure the significant sources of error. A secondary objective was to determine the impact of various levels of flight-deck automation on trajectory predictability. The results were intended to support several research and development activities including the following:

- 1) improvements to ATM and FMS prediction algorithms;
- 2) improvements to DST-data sources (e.g., aircraft tracking and wind and temperature predictions); and
- 3) development of trajectory-prediction-error models to support sensitivity studies for determining the statistical representation of errors [7-11], the sizing of buffers for conflict prediction, and the real-time analysis of conflict probability [12].

The Phase-I flight test focused on straight-path descents (Figure 1a) with an emphasis on the analysis of modeling errors that impact vertical-profile predictions (e.g., aircraft performance and winds and temperature aloft). The Phase-II flight test focused on complex arrival routing and evaluated a wider range of FMS capability for lateral navigation (LNAV) and vertical navigation (VNAV). The arrival route (Figure 1b) included a large turn during descent (typical for complex arrival routes and delay vectors). Lateral-prediction errors associated with such turns affect the fuel-efficiency and predictability of descent trajectories.

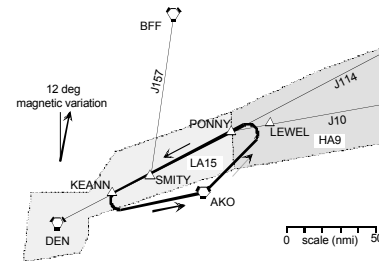


Figure 1a. Phase-I test airspace.

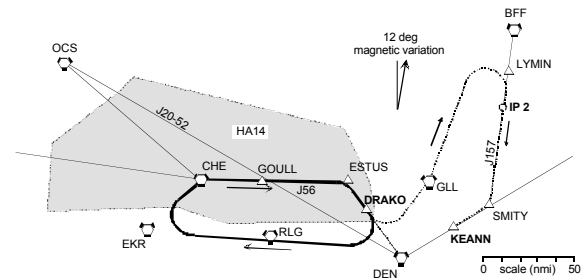


Figure 1b. Phase-II test airspace.

Approach

The tests were designed to expose EDA to realistic modeling errors with minimal impact to actual ATC and flight operations. NASA's Transport System Research Vehicle (TSRV) B737 was operated on arrival paths that replicated typical airline operations at Denver. Each test flight consisted of several test runs along a closed circuit (Figure 1). The TSRV was flown from both the forward flight deck (FFD), representing classic aircraft (e.g., B737-200), and the research flight deck (RFD), representing FMS-equipped aircraft (e.g., B737-400). Test runs were conducted during low traffic periods to allow the runs to be completed without interruption. Although interruptions commonly occur as a part of normal ATC operations,² it was desirable to isolate the TSRV to measure the worst-case error buildup and identify the magnitude of key error sources.

Experiment Set-up

Figure 2 illustrates the test setup. CTAS was operated by a test engineer. The TSRV pilot and controller coordinated pilot-discretion descents while the CTAS operator relayed EDA advisories to the TSRV by radio.

² A key EDA-benefit mechanism is the reduction of tactical (corrective) ATC clearances through the use of strategic planning that is supported by a high degree of trajectory predictability [6,7].

CTAS was operated using data sources that represent the quality of data available to a current-day operational system. Aircraft track and flight plan data were obtained from the ATC-Host computer. For the B737, CTAS used performance data from the manufacturer’s performance engineer’s manual including drag, thrust, and fuel consumption as a function of aircraft state (actual performance was a measured output of the study). Atmospheric data (winds and temperature aloft) were obtained from the National Oceanographic and Atmospheric Administration (NOAA) Mesoscale Analysis and Prognostic System (MAPS) [13].³

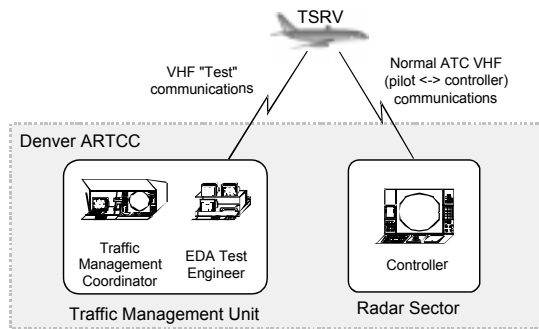


Figure 2. Flight-test set up.

Although the Phase-II tests evaluated FMS and CTAS predictions in parallel, the TSRV FMS used data from sources different from those CTAS used. Airplane-state data were taken directly from aircraft measurements. Wind profile data were manually entered into the FMS for each run based on measurements from previous runs. Performance data was calibrated from previous flight test activities. These sources were not only more accurate than those used by CTAS, the wind and performance data were even more accurate than those currently used for commercial FMS operations. This approach highlights the potential operational differences between CTAS and FMS predictions.⁴

Airplane state, winds and temperatures aloft, and the real-time FMS-trajectory predictions were recorded onboard the TSRV for later analysis. Real-time CTAS trajectory predictions, aircraft track, and MAPS data were recorded by CTAS. All data were time-tagged to Universal Time (UTC) for correlation after the flight.

TSRV Research Flight Deck.

The RFD provided the flexibility to evaluate several levels of FMS capability. The RFD was equipped with eight glass displays, a mode-control panel (MCP), and a control-display unit (CDU) to interface with the FMS computer (Figure 3). Both pilot positions were provided with their own CDU, primary flight display (PFD) and navigation display (ND). The ND included a typical range-altitude arc to project the climb or descent intercept of a target altitude (Figure 4). For Phase-II, a special “along-path” altitude marker was also displayed

to correct the projection for turns during climb or descent. The MCP and four supporting displays (engine/system monitoring) were located between the pilot positions. Detailed descriptions of the TSRV FMS and pilot displays and interface are provided in [14].



Figure 3. TSRV research flight deck.



Figure 4. TSRV navigation display (ND).

Phase-I Test Conditions

The Phase-I test employed two procedures: (1) idle descents, and (2) constrained descents. For idle-descent cases,⁵ the pilot closed the throttle at the CTAS-advised top-of-descent (TOD) and maintained the CTAS-advised speed profile using pitch. Near the bottom-of-descent (BOD) altitude, the pilot leveled off and decelerated to the meter-fix-crossing speed (250 knots or less).

Although constrained descents are initiated in a manner similar to idle descents, the pilot adjusts thrust or speed brake during the descent to conform with BOD-crossing restrictions (i.e., altitude and speed at the meter fix). Constrained descents represent a more operationally-realistic procedure that effectively mitigates the impact of trajectory-prediction errors on the descent profile. A detailed description of all Phase-I and -II descent procedures may be found in [14].

Test Matrix. The test matrix (Table 1) was designed to evaluate CTAS accuracy over the nominal speed envelope of the TSRV. For idle-descent cases, seven speed profiles were selected to generate a representative set of constant-speed and deceleration segments. This approach generated a balanced set of trajectory cases (for prediction-accuracy analysis) and a broad set of

³ MAPS is the research prototype version of the Rapid Update Cycle.
⁴ Prior to the flight test, CTAS was validated against the TSRV FMS using the same input data. Differences were negligible with predicted arrival times within 2 sec and tops-of-descent within 2 nm.

⁵ The purpose of the idle-descent procedure was to provide a direct measurement of CTAS trajectory-prediction accuracy (which used an idle-descent model for the TSRV). Operational versions of CTAS match the descent procedures to individual aircraft-performance types and operating conditions (e.g., a near-idle thrust descent model is used for most jet types, and power-on models used for prop types).

data for evaluating TSRV-performance characteristics. Constrained cases were flown from both flight decks using the first three speed profiles.

Table 1. Phase-I test matrix.

Test Case	Cruise Speed	Descent Mach/CAS	Description of Procedure
1 I	Mach 0.72	0.72/280	Nom, Idle
2 I	Mach 0.76	0.76/330	Fast, Idle
3 I	220 KCAS	/220	Slow, Idle
4 I	Mach 0.76	0.76/280	Fast Crs, Nom Des
5 I	220 KCAS	/280	Slow Crs, Nom Des
6 I	Mach 0.72	0.76/310	Nom Crs, Fast Des
7 I	Mach 0.72	/240	Nom Crs, Slow Des
1 CF	Mach 0.72	0.72/280	Nom, Const. FFD
2 CF	Mach 0.76	0.76/330	Fast, Const. FFD
3 CF	220 KCAS	/220	Slow, Const. FFD
1 CR	Mach 0.72	0.72/280	Nom, Const. RFD
2 CR	Mach 0.76	0.76/330	Fast, Const. RFD
3 CR	220 KCAS	/220	Slow, Const. RFD

Knots Calibrated Airspeed (KCAS) Cruise (Crs)
 Idle-descent procedure (I) Descent (Des)
 Constrained-descent procedure (C) Nominal (Nom)

Phase-I analysis included 23 arrival runs conducted over a period of one week in October 1992. Data was collected for 12 idle-descent runs and 11 constrained-descent runs. Although the goal was to collect data for 26 runs (two runs per test case), 3 runs were excluded from analysis due to experimental-system failures. Weather conditions were generally good. The most significant weather condition was a strong jet stream affecting two flights (9 idle-descent runs).

Phase-II Test Conditions

The Phase-II test expanded upon Phase-I in two ways. First, the arrival routing included a large turn (60° course change) during the descent. Descents with turns were of particular interest due to the increased complexity of lateral and vertical profile tracking. Second, the test matrix was expanded to investigate the accuracy of FMS predictions and the utility of VNAV capabilities for improving predictability. Three levels of FMS capability were chosen to represent a cross-section of capabilities available on current airplanes:

- 1) Classic aircraft (without FMS)
- 2) FMS-equipped with VNAV capability
- 3) FMS-equipped with range-altitude arc capability.

Four sets of pilot procedures were developed for the TSRV to take advantage of these levels of FMS automation. The names of these four procedures follow:

- 1) Classic (Non-FMS)
- 2) Conventional FMS (using the FMS TOD)
- 3) FMS with CTAS TOD
- 4) Navigation-Display (ND) Arc.

These procedures mimic the techniques proposed for use by airline-flight crews to follow CTAS descent advisories. The Non-FMS procedure was flown from the FFD, the latter three “FMS” procedures, from the RFD. All of these procedures called for the pilot to

follow the descent-speed profile while monitoring and ensuring conformance with the BOD-crossing restrictions. An investigation of operational procedures and flight-crew human factors is presented in [15].

Classic (Non-FMS). These procedures evolved from the Phase-I constrained-descent procedures. Very-high frequency Omni-range Receiver (VOR) guidance provided lateral tracking. For the vertical profile, the pilot maintained cruise altitude and speed up to the CTAS TOD. The TOD position was identified as a Distance-Measuring-Equipment (DME) range to a reference-VOR station (Denver in this case). At TOD, the pilot initiated the descent by retarding the throttle to idle. If the descent speed was less than the cruise speed, the pilot decelerated in level flight to the desired descent speed. Otherwise, the pilot pitched over and descended at the CTAS-advised Mach/CAS-speed profile. Prior to crossing 18,000 feet, the pilot updated the altimeter for the local setting. The pilots were instructed to monitor and conform to the BOD-crossing restrictions.

Conventional FMS. These descent procedures utilized the FMS capability to plan and fly a VNAV profile based on the CTAS-advised descent-speed profile. The pilot used the VNAV capability to plan and initiate the TOD independent of the CTAS-TOD advisory. These runs facilitated the comparison between the CTAS and FMS TODs. All RFD-test runs were flown using the TSRV autopilot for lateral tracking of the LNAV path.

Measured wind speed, wind direction, and static-air-temperature data were manually recorded at 4,000 ft intervals during the initial climb of each flight and on subsequent descent runs. These data were manually entered into the descent-wind page of the CDU for use in the FMS-trajectory prediction. This experimental process enabled the TSRV FMS to represent the ideal case of minimum modeling error for trajectory predictions, airborne or ground-based.

FMS with CTAS TOD. This procedure, a hybrid of the first two procedures, called for the pilot to plan and fly the lateral and vertical profiles using the FMS capabilities while initiating the descent at the CTAS TOD. Although this procedure introduced a deviation from the VNAV profile near the TOD, it would offer the dual advantage of (1) a predictable TOD for controller planning and (2) VNAV guidance for accurate pilot conformance with BOD-crossing restrictions. The specific pilot procedures used to manage potential CTAS-FMS TOD differences may be found in [14].

Navigation-Display (ND) Arc. These procedures combined the CTAS TOD of the Classic (Non-FMS) case with a simple FMS capability for vertical guidance. LNAV was used for lateral-path tracking, while a simple along-path range-altitude-arc capability was used to provide vertical guidance for the BOD-crossing restriction. The goal was to explore the feasibility of a simple alternative to complex performance-based VNAV capabilities.

These procedures were similar to the Phase-I constrained-descents flown from the RFD. For Phase-II however, the TSRV-range-altitude arc was modified to

display the projected range along the LNAV path at which the airplane would reach the BOD altitude (Figure 4). Although this projected range overlapped the range-altitude arc on straight segments, this guidance accounted for the longer range along a path with turns. This guidance helped the pilot to more accurately target the BOD location during the early stages of the descent.

Test Matrix. The Phase-II test involved 12 cases, based on three speed profiles and four pilot procedures (Table 2), with the goal of completing two runs of each case.

Table 2. Phase-II test matrix

Test Case	Speed Profile CRS / DES	FMS/Automation	Flight Deck
1 A	0.72 / 0.72/280	Classic (Non-FMS) VOR/DME CTAS TOD	FFD
2 A	0.76 / 0.76/240		
3 A	0.76 / 0.76/320		
1 B	0.72 / 0.72/280	Conventional FMS LNAV VNAV	RFD
2 B	0.76 / 0.76/240		
3 B	0.76 / 0.76/320		
1 C	0.72 / 0.72/280	FMS w/ CTAS TOD LNAV CTAS TOD & VNAV	RFD
2 C	0.76 / 0.76/240		
3 C	0.76 / 0.76/320		
1 D	0.72 / 0.72/280	Nav Display (ND) Arc LNAV CTAS TOD & ND-Arc	RFD
2 D	0.76 / 0.76/240		
3 D	0.76 / 0.76/320		

Phase-II analysis included 25 arrival runs conducted during 9 daytime flights over a period of one week in September 1994. Two runs were collected for each case (with the exception of 3 runs for case 2B). A variety of weather conditions were encountered. Light winds and stable conditions prevailed during the first two days of testing (10 runs). Convective buildups and stronger winds (approximately 60 knots at cruise) were encountered on the third day of testing (6 runs) with storm cells and light rain in the vicinity of the descent turn. Good weather prevailed for the fourth day of testing (3 runs). The fifth day (3 runs) encountered a frontal passage that introduced strong and variable winds aloft (80-90 knots) and snowstorms throughout Colorado that forced the termination of that flight. The strong winds continued for the final day of testing (3 runs) with clear conditions. High pressure dominated the area throughout the test with altimeter settings that were above standard each day (a characteristic that exacerbated a system error described in a later section).

Results and Discussion

The flight-test results are presented in three sections: Error Sources and Magnitudes, 4D Trajectory-Prediction Accuracy (CTAS and FMS), and CTAS Arrival-Time-Error Accounting. The first section presents the analysis of error components that, in combination, lead directly to the observed trajectory-prediction errors described next. The authors chose this order of presentation to facilitate the understanding of the observed 4D trajectory-prediction-accuracy results in the second section. The third section then provides a complementary analysis of the trajectory-prediction errors by accounting for the contribution of each error source to the total observed

error (i.e., how much time error was due to wind-prediction error as opposed to performance-model error and other sources). Due to limitations in the scope of this paper, error-accounting results will only be presented for the meter-fix arrival-time-error results.

Error Sources and Magnitudes

The five main CTAS error sources encountered were (1) Radar Tracking Errors, (2) Airplane Performance Model Errors, (3) Atmospheric Modeling Errors, errors in (4) Pilot Conformance, and (5) Experimental System Errors.

Radar-Tracking Errors. Errors in estimated position and velocity were analyzed by comparing the radar track and GPS data across all runs. The along-track-position error (at the initial condition for the CTAS predictions) had a mean less than 1.0 nm with a standard deviation less than 0.5 nm for both test phases.⁶ The corresponding cross-track errors displayed means and standard deviations below 0.2 nm.⁷ From a controller's point of view regarding the separation and spacing of flights, this mean along-track error is essentially a systematic bias that cancels itself out⁸ while the standard deviation would add to the uncertainty in separating any two flights.

The ground-speed errors at the CTAS initial conditions resulted in mean errors less than 5 knots with standard deviations less than 7 knots for both phases. The mean initial track-angle errors were within 3 deg with standard deviations less than 6 deg. Significant transient errors in the tracker were also observed (e.g., associated with turns) but did not impact the test results [14]. A total of 45 Phase-II turns were analyzed, ranging from 3° to 305° with a mean turn angle of 68°. The ground-speed error varied with turn size, often exceeding 100 knots, with a mean of 37 knots during the actual turn maneuver. Following the turn, it took an average of 93 sec for the ground-speed error to drop below 10 knots. The mean error during these transient periods was 59 knots. Although the mean track-angle errors were relatively small, the standard deviation during actual turns was 28°. These transient velocity-estimation errors, even though occasional, could be problematic for ATM-DST applications if they are not reduced in size by improved surveillance systems.

Airplane-Performance-Model Errors. Analysis of flight-test data indicated that the actual TSRV drag was 11% greater than modeled [14]. The actual idle-thrust was also greater than modeled, yielding an average of 5% error in net thrust-minus-drag over the descent. For Phase-II, CTAS used the published performance data while the TSRV FMS used the actual performance data. CTAS modeled the weight of the TSRV with a typical descent weight of 85,000 lb, while the FMS model used

⁶ One nmi of along-track error in the initial condition was approximately equivalent to 6.4 seconds of time error for these tests.

⁷ The along-track error was primarily due to the lack of a Host time stamp. The CTAS-estimated time stamp may be up to 12 sec off (the period of one Host track-update cycle).

⁸ From an air-ground trajectory-exchange point of view, the mean along-track error would affect trajectory-prediction accuracy also.

the actual weight of the TSRV (averaging 83,560 lbs with a standard deviation of 4380 lbs during test runs).

Atmospheric Modeling Errors. CTAS accuracy depends, in large part, on the accuracy of the predicted atmospheric characteristics (winds and temperature aloft). Winds and temperature form the basis for ground-speed-profile predictions related to CTAS speed advisories. Winds are also critical in estimating airspeed from radar-based ground-speed. Wind gradient (with respect to altitude) directly influences the rate of climb and descent. Temperature profiles and altimeter settings are used to correct airplane performance for non-standard atmospheric conditions.

Atmospheric modeling errors were analyzed by comparing TSRV measurements with the CTAS-interpolated values at specific altitudes along each flight. General results are summarized here; detailed results may be found in [14, 16].

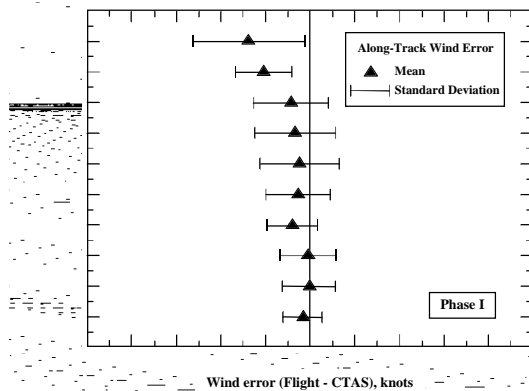


Figure 5a. Aggregate CTAS wind error, Phase-I.

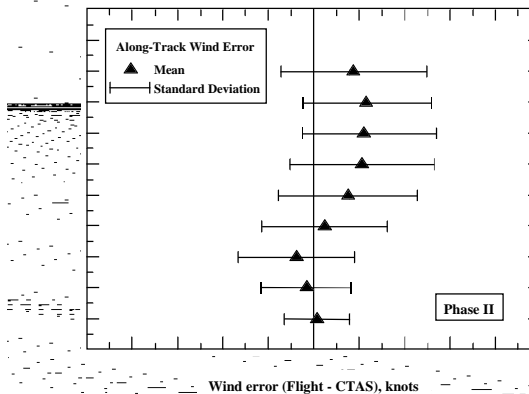


Figure 5b. Aggregate CTAS wind error, Phase-II.

Over both test phases, temperatures tended to be warmer than standard with a larger altitude gradient (lapse rate). Mean values ranged from 8-9° C above standard, at lower altitudes (17,000 ft), to 2° C above standard, at cruise altitudes. Mean errors were approximately 3° C in Phase-I and 1° C in Phase-II.

The accuracy of predicted winds was not as good as that of temperatures. Figure 5 presents a composite of wind errors as a function of altitude. Although the mean of the predicted wind errors tended to be much smaller at the lower altitudes, the standard deviation at all altitudes was still quite large (10-20 knots). In fact, the wind error at cruise approached 80 knots for several

Phase-II runs. Results from these tests revealed the occasional existence of “large” errors in the predicted wind field (greater than 20 knots) that span multiple sectors for periods greater than several hours at a time.⁹ Further analyses of the wind errors revealed that an error in the CTAS wind-interpolation scheme (since corrected) contributed about 30% of the total error [17].

In Phase II, the wind data that was hand-collected and entered into the FMS, for each FMS run, was much more accurate than the CTAS data. Figure 6 shows the mean differences between measured winds and those entered into the FMS for Phase-II flights. The standard deviation of the FMS wind error was approximately half as large as that of the CTAS wind error [14]. This data is used to support the analysis of the TSRV FMS-based trajectory predictions in the next section.

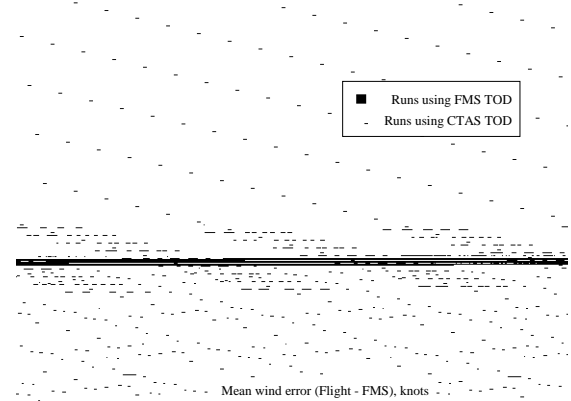


Figure 6. Mean FMS along-track wind error, Phase-II.

Pilot Conformance. These errors represent the accuracy of pilot conformance with airspeed, TOD, and route clearances. The TSRV pilots were able to maintain speed within 1% (mean) of the clearance speed with a standard deviation less than 2% (Table 3). For the runs using CTAS-TOD procedures, the mean TOD error was 0.9 nm late (i.e., actual TOD was downstream of the CTAS TOD) with a standard deviation of 0.8 nm.

Table 3. Pilot conformance to speed clearances.

Speed Profile	Phase-I			
	FFD		RFD	
	Mean	Std dev	Mean	Std dev
Cruise, Mach	0.005	0.009	0.001	0.003
Descent, Mach	0.008	0.007	0.001	0.009
Descent, KCAS	-0.9	3.4	-0.2	3.1

Speed Profile	Phase-II			
	FFD		RFD	
	Mean	Std dev	Mean	Std dev
Cruise, Mach	0.010	0.007	0.001	0.004
Descent, Mach	0.009	0.008	0.004	0.008
Descent, KCAS	1.5	5.5	0.3	4.8

Lateral-path errors were not a factor for the straight-path descents in Phase-I. For Phase-II however, the Classic cases (VOR-radial tracking) did experience lateral-path deviations that generated notable along-track and cross-track error. During these runs, the pilots

⁹ A 13-month study of Denver airspace confirmed this phenomenon and validated two approaches that significantly reduce this error [16].

tracked the VOR radials as precisely as possible, and were generally within one needle-width of the outbound radial from the Hayden (CHE) VOR (Figure 1b). Lateral-path deviations of greater than one mile occurred during and after the turn at ESTUS even though the pilots were using the flight director and course-deviation indicator (CDI) to their best advantage. Although no data was recorded on CDI deflection, actual cross-track error was recorded and is examined in a following section.

Experimental-System Errors. These errors are uniquely attributable to the experimental nature of the CTAS and TSRV field-test systems and would not be characteristic of operational systems. Where possible, appropriate corrections were made to the 4D accuracy analysis presented in the next section; where not possible, the impact of these errors on the results is described.

During Phase-I, a computational error in the CTAS trajectory-generation code inadvertently nulled the wind-gradient component of the descent-rate computations. Phase-I runs encountered along-track gradients ranging from 0-4 knots/1000 ft. Off-line analyses of the TSRV airplane indicated that each 1 knot/1000 ft error in the along-track-wind gradient contributed an approximately 3.5% error to the descent rate. This CTAS bug was corrected prior to Phase-II.

Several different problems affected Phase-II data. First, a routine FAA update to the radar-coordinate-system adaptation occurred during the test. Unfortunately, this information was not updated in the CTAS adaptation database. This resulted in a CTAS initial position error of approximately 1.5 nm for all of the runs. Post-test analysis corrected for this error by adjusting the process used to correlate track data with recordings of the predicted trajectories.

The second error affected the CTAS initial-speed estimate for three Phase-II runs. At the time of the test, CTAS synthesized cruise segments for arrivals via backward integration from the predicted TOD (as opposed to the current technique of forward integration from the flight's initial speed estimate). An error in the wind-interpolation scheme (since corrected) artificially introduced a large difference between the predicted ground-speed in cruise and the radar-track-based estimate. This error directly affected the time-profile-error results discussed in the next section.

A third error affected the CTAS model for non-standard atmospheric conditions. A sign error in the correction for the local altimeter setting (since corrected) introduced a 400-800 ft error in the predicted BOD altitude for all Phase-II runs. The higher-than-standard altimeter settings resulted in a CTAS prediction of BOD altitude that was higher than actual.

The final CTAS-system error involved a bug in flight-plan processing. Later analysis revealed that flight-plan amendments (routinely made by the controllers between TSRV runs) triggered CTAS to assign an incorrect airplane model to the TSRV. Although the incorrect model (the commercial variant of the B737) contained identical thrust and drag data, the nominal descent weight modeled by CTAS was 13,000 lb heavier. This

heavier weight resulted in shallower descent-profile predictions for the runs affected.

One experimental-system error affected the TSRV FMS vertical-profile predictions. An unintended software "feature" incorrectly led to an excessively large (5000 ft) integration-step size for descent segments. Compared with a nominal setting of 500 ft, the larger vertical step size resulted in a significant error in the estimation of the along-path winds. This error artificially contributed to the difference between the CTAS and FMS prediction results presented in the next section.

4D Trajectory Prediction Accuracy

The CTAS and FMS trajectory predictions were compared with the actual path as measured by the TSRV. Each 4D trajectory was decomposed into four component 2D profiles: (1) Cross-Track, (2) Along-Track, (3) Altitude, and (4) Time. Each 2D profile was formed by correlating the profile parameter (e.g., cross-track) with a common reference path defined by the predicted trajectory. Analysis was performed at trajectory "gates" corresponding to vertical-profile events (i.e., the initial condition, TOD, intermediate altitudes, BOD, and meter fix). This decomposition facilitated the analysis and presentation of results across all the runs. For the purposes of this paper, errors are defined as negative if the aircraft reaches a given state earlier (in time) or further upstream (along path) than was predicted. For the errors presented in the following sections, this corresponds to the sign convention of "actual minus predicted."

Cross-Track Profile. Results for Phase-II are illustrated in Figure 7.¹⁰ Although the lateral error for the LNAV assisted runs was negligible, the Classic (Non-FMS) runs exhibited a significant error consistent with the findings in [2]. Figure 8 illustrates several example lateral profiles for Classic (Non-FMS) runs. Prior to the turn, errors in VOR-radial tracking resulted in a mean "offset" of nearly 1 nm (left of course) with a standard deviation of approximately the same size. Additional error, resulting from turn overshoot, essentially doubled the cross-track error following the turn.

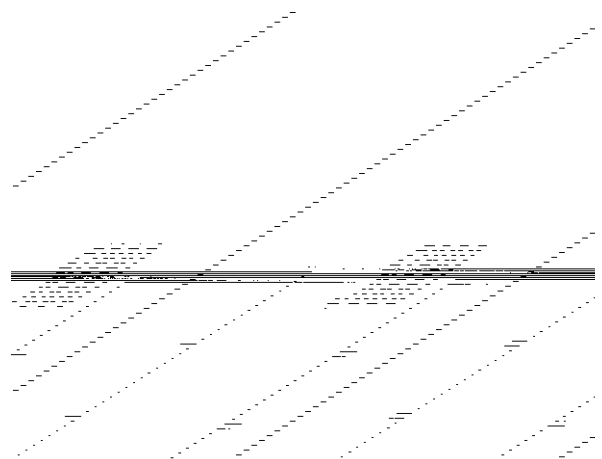


Figure 7. Cross-track error, Phase-II.

¹⁰ For brevity, only Phase-II results are presented since cross-track error had a negligible impact on Phase-I results.

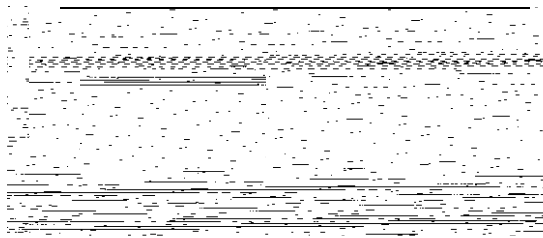


Figure 8. Sample (Non-FMS) lateral paths, Phase-II.

Along-Track Profile. Figure 9 presents the along-track profile error. As in the cross-track profile, the error associated with the LNAV runs was negligible (primarily because of the cross-track accuracy). The figure also illustrates the CTAS accuracy in predicting the path of the turn. However, the cross-track error for the Non-FMS runs, coupled with the turn overshoot, resulted in a significant increase in distance flown. The cumulative effect of cross-track errors added a mean of 1.3 nm to the path length with a standard deviation of 1.1 nm.

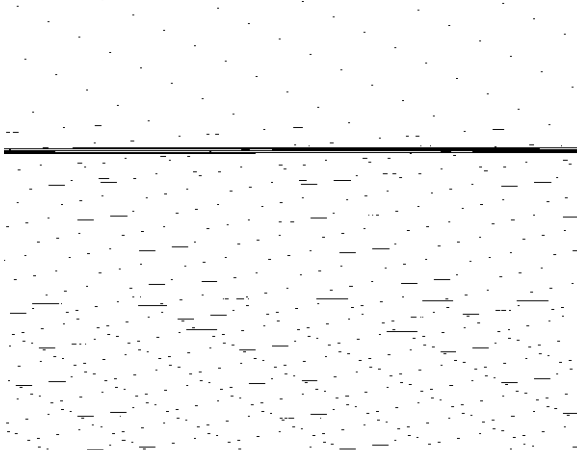


Figure 9. Along-track error, Phase-II.

Altitude Profile. Figure 10 presents the Phase-I altitude-profile results. Both procedures began similarly with a slight error after TOD due to a 1 nm round-off of the CTAS TOD advisory and unmodeled transients in the pilot's pitch-over and throttle reduction. The TSRV then descended approximately 15% steeper than predicted. This error was primarily due to errors in the CTAS performance model (5%) and the wind-gradient bug (7%). Actual wind gradients during Phase-I averaged 2 knots/1000 ft. The largest altitude error occurred near the bottom of the descent with a mean of just over 1500 ft and standard deviation of 900 ft. Compared with idle-descent cases, constrained-descent procedures reduced the maximum error by 50%.

The altitude-profile results for Phase-II were more complex (Figure 11). For the Non-FMS runs, the flights slightly overshoot the CTAS TOD and began the descent above path. During descent, the mean error fell below the CTAS-predicted path (primarily due to performance and wind-modeling error). The error growth then increased at the lower altitudes following the turn (below FL250).¹¹ The error then dropped off as the TSRV approached the BOD altitude. The final error at the meter fix (for all

¹¹ The turn overshoot contributed approximately 400 ft (below path) to the mean altitude error with a standard deviation of about 370 ft.

runs) was due entirely to the systematic experimental error in the CTAS altimeter-setting correction.

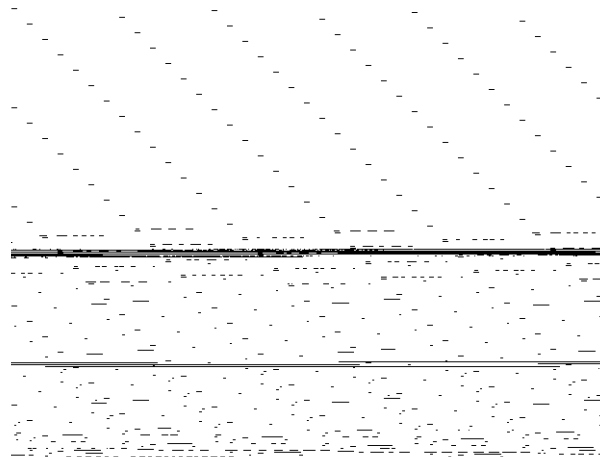


Figure 10. Altitude-profile error, Phase-I.

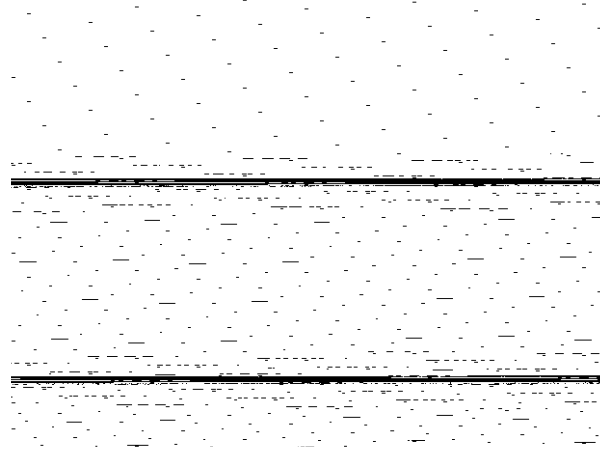


Figure 11. Altitude-profile error, Phase-II.

In comparison, the FMS cases (FMS and CTAS TOD) exhibited a large “above path” error just after TOD that monotonically reduced (in both mean and standard deviation) toward the BOD. This error was due to differences between the FMS and CTAS vertical-profile predictions. Performance model differences and experimental errors tended to make the FMS-predicted paths steeper than CTAS. The FMS-computed TOD was 2.5 nm later than the CTAS-predicted TOD, on average, with a standard deviation of 2.8 nm. Even with these differences, the FMS vertical guidance dramatically reduced the altitude error over the descent.

A comparison between FMS cases reveals a significant difference in vertical-profile error. The mean error for the CTAS-TOD procedure was approximately 500 ft larger (above the CTAS path) for intermediate descent altitudes. This difference was not caused by the procedure *per se*, but was due to other factors coincident with the runs (i.e., variation in both the wind error and effect of the experimental system error on the TSRV-FMS vertical-profile integration). Except at the top-of-descent, where the CTAS-TOD procedure mitigated differences between the FMS and CTAS predictions, both FMS cases used the FMS vertical path.

Similar to the Non-FMS runs, the ND-Arc runs also exhibited an initial growth in mean error (below the CTAS path) following the TOD. However, as the

TSRV descended, the error growth was reversed as the pilots used the ND-Arc guidance to control the BOD.

Time Profile. The critical output of 4D predictions is the along-track-time profile. The results presented here reflect adjustments that removed the influence of radar-track-position errors and the Phase-II experimental coordinate-system error. Application of these results for conflict-probability analysis, or the sizing of separation buffers, must account for the additional uncertainty due to radar-track-position error. A supporting analysis of speed-profile error is provided in [14].

Phase-I time-error-profile results are presented in Figure 12. Both the idle and constrained cases have similar profiles prior to the middle of descent, followed by a reduction in time-error growth associated with the constrained cases (due to their reduced vertical-profile error, as illustrated in Figure 10).

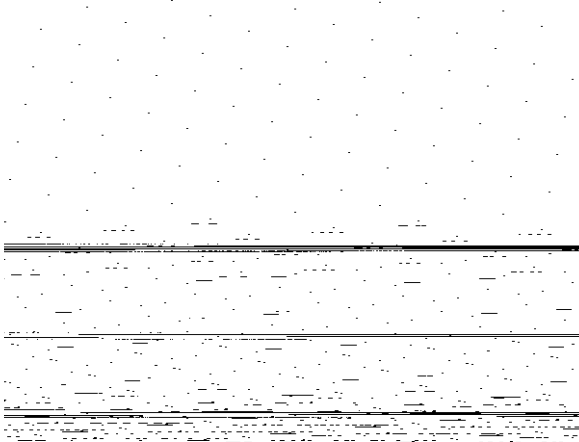


Figure 12. Phase-I time-profile error.

Phase-I meter-fix-time-error results are summarized in Table 4. The time error for all runs was less than 17 sec in mean and 15 sec in standard deviation. For the idle-descent cases, additional analysis indicated that wind-prediction error accounted for approximately 70% of the mean error and nearly all of the standard deviation [14]. The remainder of the mean error was primarily due to errors in the CTAS performance model.¹² Compared with idle descents, the constrained procedures were expected to be more accurate due to the procedure's mitigation of vertical-profile error. The RFD-constrained cases did reduce the mean error by 40% and standard deviation by 33%. However, problems related to FFD-constrained-procedure training led to less favorable results.¹³

Arrival-time-accuracy results for Phase-II are presented in Table 5 for both CTAS and FMS predictions.¹⁴ Results for CTAS predictions will be discussed first, followed by results related to the FMS-predictions.

Overall, the CTAS arrival-time error for all Phase-II runs was within 10 seconds in mean and 14 seconds in standard

¹² Although performance-model error has a small impact on descent-prediction accuracy the impact on ascent predictions will be large.

¹³ A training error led to premature deceleration at BOD. Lessons learned led to improvements that prevented this problem in Phase II.

¹⁴ Comparison of CTAS and FMS accuracy should be restricted to Conventional FMS and FMS-with-CTAS-TOD runs only. The other cases did not use the FMS-VNAV path for guidance.

deviation. A comparison of Tables 4 and 5 shows an interesting shift in the mean CTAS arrival-time error. While the TSRV tended to arrive later than predicted in Phase-I, it arrived earlier than predicted in Phase-II. This result was due to a combination of wind-prediction error and course that led to a stronger headwind (than predicted) in Phase-I, and a stronger tailwind in Phase-II.

Table 4. Phase-I meter-fix arrival-time error.

Procedure Case	Time error, sec	
	Mean	Std. dev.
Idle descent	16.6	9.9
Constrained (RFD)	9.9	6.4
Constrained (FFD)	16.4	14.8

Table 5. Phase-II meter-fix arrival-time error.

Procedure Case	Time error, sec			
	CTAS		FMS	
	Mean	Std. dev.	Mean	Std. dev.
Non-FMS	1.9	8.7		
Conventional FMS	- 4.6	13.9	2.0	11.3
FMS w/ CTAS TOD	- 9.9	10.2	2.8	4.4
ND-Arc	2.3	13.8		
All runs	- 2.7	12.3		

Considering the Phase-II CTAS results alone (Table 5), it was surprising to find a smaller error for the Non-FMS case compared to the three other FMS-related cases. The three FMS-related cases were expected to have less error due to the advantages of lateral and vertical guidance. Further time-profile analysis (Figure 13) revealed the following. For the Non-FMS case, the mean error grew rapidly until midway through the descent (15 sec early), and then fell off to end up 2 sec late at the meter fix. This reversal was due to compensating errors that included a stronger tailwind (than predicted) and turn overshoot. If the results are adjusted to remove the turn-overshoot effect, the net arrival-time error would be -11.0 sec mean (i.e., early) with a standard deviation of 15.5 sec. Compared to these adjusted results, the FMS-related cases resulted in less time error due to their mitigation of vertical error. The ND-Arc case showed comparable accuracy without requiring performance-based VNAV capability.

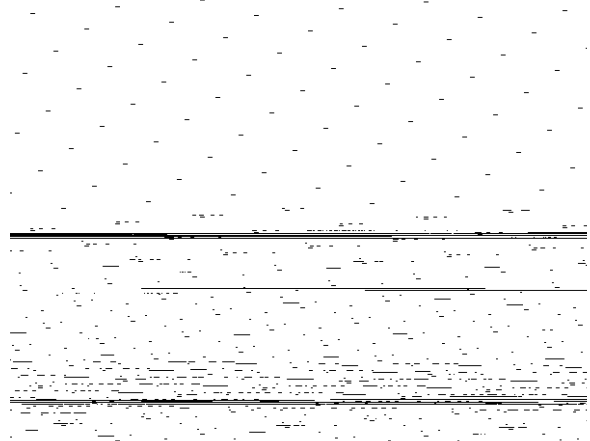


Figure 13. Phase-II time-profile error.

Table 5 also presents time-error results for the TSRV-FMS predictions for the two VNAV procedures flown.

The primary factor contributing to the differences between the FMS and CTAS predictions was the source of wind data. Compared to the CTAS predictions, the mean along-track-wind errors were significantly lower for the FMS predictions (Figures 5 and 6), resulting in a lower mean arrival-time error. Further analysis showed that the difference in standard deviation between the FMS-prediction cases was primarily due to a coincidental difference in the standard deviation of along-track-wind error between the two cases (approximately 9 knots for the Conventional-FMS case and 4 knots for the FMS-with-CTAS-TOD case) [14].

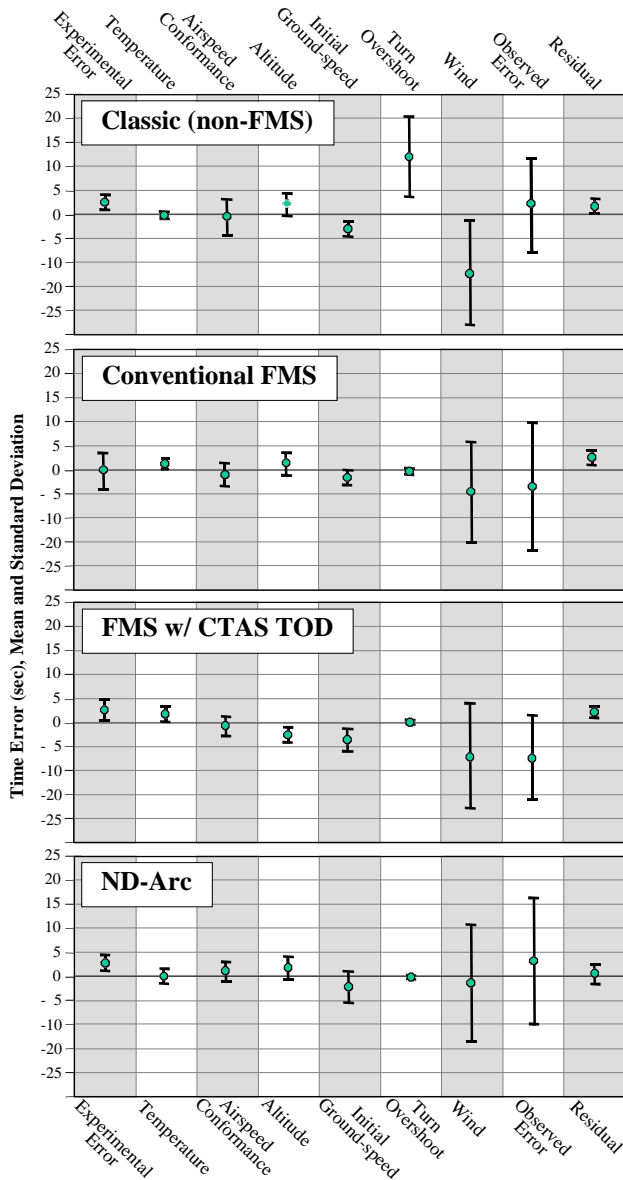


Figure 14. Arrival-time-error accounting

CTAS Arrival-Time-Error Accounting

Additional Phase-II analysis provides an accounting of CTAS arrival-time error as a function of error sources. This breakdown of the impact of individual error sources is presented to facilitate deeper analysis and insights that may extend the modest sample size to a more significant representation of real-world CTAS trajectory-prediction-accuracy performance. For the purposes of this paper, results are presented for arrival-

time error only (Figure 14). The top seven error sources are represented. The two right-most columns present the observed errors (Table 5) and the residual error that was not accounted for by the seven sources.

Figure 14 clearly illustrates the dominance of wind-prediction errors on CTAS trajectory prediction (third column from the right). However, for the classic (Non-FMS) runs, another dominant factor, turn overshoot, compensated for the winds, resulting in a remarkably small net arrival-time error. The figure also indicates that although the experimental system errors combined to contribute a visible effect on the vertical-profile predictions (Figure 11), the impact on arrival-time error was not significant. In general, the cases involving FMS vertical guidance were dominated by wind error (the LNAV capability clearly eliminated the turn-overshoot error). For the ND-Arc runs, however, the combined effects of the “below path” altitude error (due to errors in the CTAS performance model) and experimental errors did provide a modest influence, pulling the observed arrival-time error slightly late of on time.

In summary, improvements in wind-prediction accuracy and lateral navigation capability will substantially improve CTAS arrival-time-prediction accuracy.

Concluding Remarks

Two flight tests were conducted at Denver Center to evaluate the en route descent-prediction accuracy and error sources associated with ground-based and airborne automation systems. A total of 48 trajectories were analyzed including 23 straight-path-descent runs (Phase-I) and 25 descents with turns (Phase-II).

The CTAS arrival-time error for all Phase-I runs was measured to have a mean of 14.7 sec (late) with a standard deviation of 9.6 sec. Analysis indicated that wind errors accounted for approximately two-thirds of the mean time error and nearly all of the standard deviation. The remaining error was primarily due to errors in the vertical-profile prediction. Constrained-descent procedures, compared with idle procedures, reduced the maximum vertical-profile error by 50% (approximately 750 ft). Use of FMS-like range-altitude guidance reduced the mean time error from 16.6 sec to 9.9 sec, and the standard deviation from 9.9 to 6.4 sec.

The CTAS arrival-time error for all Phase-II runs was measured to have a mean of 2.7 sec (i.e., early) with a standard deviation of 12.3 sec. Classic (Non-FMS) aircraft runs appeared to have the smallest time error with a mean of 1.9 sec (late) and a standard deviation of 8.7 sec, but this result was due to a coincidental canceling of the primary error sources (turn overshoot, related to conventional VOR-route guidance, and wind-prediction error). Turn overshoot contributed a mean error of 12 sec (late) with a standard deviation of 9 sec. Wind error contributed a mean of -12 sec (i.e., early) with a standard deviation of 11 sec. Secondary error sources, including the initial ground-speed (due to tracker error), altitude profile (due to model error), and experimental error, each contributed 3 sec or less to the mean error.

CTAS results for Conventional-FMS runs indicated a mean error of -4.6 sec (i.e., early) with a standard deviation of 13.9 sec. Wind-prediction errors were dominant, with a mean error contribution of -5 sec (i.e., early) and a standard deviation of 11 sec. Secondary error sources included the initial ground-speed, altitude profile, and experimental errors. Although the FMS-with-CTAS-TOD runs resulted in a larger mean error and smaller standard deviation than the other FMS cases, the difference was due to a coincidental combination of the secondary error sources. For all FMS-related cases, the LNAV guidance prevented turn-overshoot error while the VNAV guidance significantly reduced the vertical-profile error towards the bottom-of-descent.

The ND-Arc runs demonstrated many of the advantages of the other FMS cases without the complexity of a performance-based VNAV system. Although the standard deviation in arrival time error was similar to the other FMS cases, the mean error was smaller (2.3 sec late) because of a coincidentally smaller mean wind-error. The errors in initial ground-speed and altitude profile were secondary factors. As in the other FMS cases, the use of LNAV prevented overshoot error; and the simple range-altitude guidance minimized the altitude error at both the top- and bottom-of-descent.

Overall, temperature and airspeed errors contributed very little to time error. Although a measured 5% error in the CTAS airplane-performance-model did contribute to vertical-profile prediction error, the impact on the time profile was small. ATC radar-track position and velocity estimates also had a negligible impact on the results of these tests. However, observations of tracker performance revealed transient ground-speed errors that exceeded 100 knots and persisted for up to 3 minutes following a turn. Such errors may render the tracker data useless for DST predictions during turns. Although several experimental-system errors did impact CTAS and FMS vertical-prediction accuracy, their effect was isolated through analysis and their overall contribution to time-profile accuracy was found to be small.

The FMS predictions demonstrated better arrival-time accuracy than the CTAS predictions. However, this advantage was due to the more accurate data inputs made available to the TSRV FMS during these tests. Although an FMS prediction may have access to better performance-model data, the superior accuracy demonstrated by the TSRV FMS in these tests is almost entirely due to better wind data (as opposed to any algorithmic differences between CTAS and FMS predictions). In fact, the hand-entered FMS wind-data used in this test removed much of the wind error that would be associated with operational FMS use today.

Future research activities will focus on the validation of climb-prediction accuracy, and the validation and enhancement of operational wind-prediction products.

References

- 1) Green, S.M., Davis, T.J., and Erzberger, H., "A Piloted Simulator Evaluation of a Ground-Based 4D Descent Advisor Algorithm," AIAA-87-252, AIAA Conference on Guidance, Navigation, and Control, Monterey, CA, Aug. 1987.
- 2) Davis, T.J., and Green, S.M., "Piloted Simulation of a Ground-Based Time-Control Concept for Air Traffic Control." NASA TM-101085, Jun. 1989.
- 3) Erzberger, H., Davis, T.J., and Green, S.M., "Design of Center-TRACON Automation System," Proceedings of the AGARD Guidance and Control Panel 56th Symposium on Machine Intelligence in Air Traffic Management, Berlin, Germany, 1993.
- 4) Green, S., "EDA Concept Definition, NASA AATT Milestone 5.10," AATT Project Office, NASA Ames Research Center, Moffett Field, CA 94035, Sep. 1999.
- 5) Jardin, M. and Erzberger, H., "Atmospheric Data Acquisition and Interpolation for Enhanced Trajectory Prediction Accuracy in the Center-TRACON Automation System," AIAA-96-0271.
- 6) Slattery, R. and Zhao, Y., "Trajectory Synthesis for Air Traffic Automation," AIAA Journal of Guidance, Control, and Dynamics, Vol. 20, No.2 Mar.-Apr. 1997.
- 7) Hunter, G., et. al., "CTAS Error Sensitivity, Fuel Efficiency, and Throughput Benefits Analysis," Seagull Technology TR96150-02, Jul. 1996.
- 8) Couluris, G., Weidner, T., Hunter, G., "Initial Air Traffic Management (ATM) Enhancement Potential Benefits Analysis." Sub-contract Report 96151-01 to Crown Communications, Inc., FAA Contract No. C010 (DTFA01-96-Y-01009), Sep. 1996.
- 9) Jackson, M., "Sensitivity of Trajectory Prediction in Air Traffic and Flight Management Systems" Ph.D. dissertation, University of Minnesota, 1998.
- 10) Weidner, T., Davidson, G., Coppenbarger, R. and Green, S., "Modeling of ATM Interruption Benefits," AIAA-99-4296, AIAA Guidance, Navigation, and Control Conference, Portland, OR, Aug. 1999.
- 11) Weidner, T., and Green, S., "Modeling of ATM CD&R and Metering Conformance Benefits," 3rd USA / EUROCONTROL Air Traffic Management R&D Seminar, Naples Italy, Jun. 2000.
- 12) Erzberger, H., et. al., "Conflict Detection and Resolution In the Presence of Prediction Error," 1st USA / Europe Air Traffic Management R&D Seminar, Saclay, France, Jun. 1997.
- 13) Benjamin, S. G., et al., "The Rapid Update Cycle at NMC." Preprints, Tenth Conference on Numerical Weather Prediction, Portland, OR, American Meteorological Society, 1994.
- 14) Williams, D., Green, S., "Flight Evaluation of CTAS Trajectory Prediction Process", NASA TP-1998-208439, Jul. 1998.
- 15) Palmer, E., et al.: "Field Evaluation of Flight Deck Procedures for Flying CTAS Descents," Presented at the Ninth International Symposium on Aviation Psychology, Columbus, OH, Apr. 1997.
- 16) Cole, R., et. al., "Wind Prediction Accuracy for Air Traffic Management Decision Support Tools," 3rd USA / EUROCONTROL Air Traffic Management R&D Seminar, Naples Italy, Jun. 2000.
- 17) Jardin, M. and Green, S., "Atmospheric Data Error Analysis for the 1994 CTAS Descent Advisor Preliminary Field Test", NASA TM-1998-112228.